Targeting Metastable Coiled-Coil Domains by Computational Design

3 AUTHORS, INCLUDING:

Patrick Barth
Baylor College of Medicine
22 PUBLICATIONS **1,263** CITATIONS

Targeting Metastable Coiled-Coil Domains by Computational Design

Patrick Barth,*,† Allyn Schoeffler, and Tom Alber

Department of Molecular and Cell Biology, University of California, Berkeley, CA 94720-3220

Received April 9, 2008; E-mail: barthp@u.washington.edu

Abstract: Approximately 30% of eukaryotic genomes are predicted to encode partially unfolded proteins. Many of these unstructured domains contact multiple partners in short-lived interactions critical for cellular homeostasis. Understanding the functional implications of these transient binding events is a current challenge that could be addressed with designed peptide inhibitors. Most current protein design methodologies, however, target only structurally well-defined, stable structures. To address this limitation, we implemented a computational design strategy that alternates between a fixed backbone sequence search for binding specificity and structural optimization of the designed interfaces. We applied this method to create specific peptide inhibitors of the C-terminal metastable coiled-coil domain of the essential yeast septin Cdc12p. Specific binding of the designed sequences was demonstrated by circular dichroism and equilibrium ultracentrifugation. Our results validate computational methods to design specific peptide ligands to protein domains lacking intrinsic structural stability and set the stage for functional analysis of Cdc12p coiled coil function *in vivo*.

Introduction

The coiled coil is a widespread recognition motif predicted from sequence analysis to be encoded by 3−5% of amino-acids in proteins.[1] The parallel coiled coil is probably the simplest protein−protein interface, and it has been studied extensively as a model system for molecular recognition. The hallmark of the coiled coil is a seven-residue sequence repeat (with positions named a−g) containing small hydrophobic residues in the first (a) and fourth (d) positions. In addition, large polar or oppositely charged residues often occur in positions e and g. As highlighted by the structure of the GCN4 coiled coil,[2] hydrophobic residues (e.g., Val, Leu, Ile) at a and d establish the hydrophobic core of the interface, and charged residues at the g and succeeding e positions form complementary electrostatic interactions across the binding interface. This simplicity has allowed a diverse range of engineering approaches, such as sequence-based design,[3] *in vivo* evolution,[4] rational design,[5−7] and computational design.[8−11]

to dissect the energetic determinants governing the stability and structural specificity of the coiled-coil motif. The regular self-assembly properties of coiled coils also have been harnessed to design new nanomaterials.[12,13] However, many coiled coils have been identified that present packing defects[14,15] or irregularities in heptad repeats.[16,17] By promoting instability and flexibility, these deviations from ideal structures are thought to provide metastability and reversible oligomerization functions to coiled coils.[14,15]

The lack of structural specificity, i.e. structural disorder, also has been recognized to be an important property of a significant fraction of protein domains in eukaryotes.[18] Many of these domains are predicted to interact transiently with several physiological partners and to play central roles in cellular control,[19] but the functional implications of these binding events are still poorly understood. Inhibition of these transient complexes *in vivo* with specific designed peptides has the potential to dissect the network of interactions involving these proteins.

† Present address: Department of Biochemistry, University of Washington, Seattle, WA 98195.

(1) Wolf, E.; Kim, P. S.; Berger, B. *Protein Sci.* **1997**, *6*, 1179–1189.
(2) O'Shea, E. K.; Klemm, J. D.; Kim, P. S.; Alber, T. *Science* **1991**, *254*, 539–544.
(3) Sharma, V. A.; Logan, J.; King, D. S.; White, R.; Alber, T. *Curr. Biol.* **1998**, *8*, 823–830.
(4) Arndt, K. M.; Pelletier, J. N.; Muller, K. M.; Alber, T.; Michnick, S. W.; Pluckthun, A. *J. Mol. Biol.* **2000**, *295*, 627–639.
(5) Harbury, P. B.; Zhang, T.; Kim, P. S.; Alber, T. *Science* **1993**, *262*, 1401–1407.
(6) Gonzalez, L., Jr.; Plecs, J. J.; Alber, T. *Nat. Struct. Biol.* **1996**, *3*, 510–515.
(7) Zhou, N. E.; Zhu, B. Y.; Kay, C. M.; Hodges, R. S. *Biopolymers* **1992**, *32*, 419–426.
(8) Harbury, P. B.; Plecs, J. J.; Tidor, B.; Alber, T.; Kim, P. S. *Science* **1998**, *282*, 1462–1467.
(9) Keating, A. E.; Malashkevich, V. N.; Tidor, B.; Kim, P. S. *Proc. Natl. Acad. Sci. U.S.A.* **2001**, *98*, 14825–14830.
(10) Havranek, J. J.; Harbury, P. B. *Nat. Struct. Biol.* **2003**, *10*, 45–52.

(11) Grigoryan, G.; Keating, A. E. *J. Mol. Biol.* **2006**, *355*, 1125–1142.
(12) Pandya, M. J.; Spooner, G. M.; Sunde, M.; Thorpe, J. R.; Rodger, A.; Woolfson, D. N. *Biochemistry* **2000**, *39*, 8728–8734.
(13) Papapostolou, D.; Smith, A. M.; Atkins, E. D.; Oliver, S. J.; Ryadnov, M. G.; Serpell, L. C.; Woolfson, D. N. *Proc. Natl. Acad. Sci. U.S.A.* **2007**, *104*, 10853–10858.
(14) Li, Y.; Brown, J. H.; Reshetnikova, L.; Blazsek, A.; Farkas, L.; Nyitray, L.; Cohen, C. *Nature* **2003**, *424*, 341–345.
(15) Shimizu, T.; Ihara, K.; Maesaki, R.; Amano, M.; Kaibuchi, K.; Hakoshima, T. *J. Biol. Chem.* **2003**, *278*, 46046–46051.
(16) Hicks, M. R.; Holberton, D. V.; Kowalczyk, C.; Woolfson, D. N. *Fold Des.* **1997**, *2*, 149–158.
(17) Hicks, M. R.; Walshaw, J.; Woolfson, D. N. *J. Struct. Biol.* **2002**, *137*, 73–81.
(18) Dyson, H. J.; Wright, P. E. *Nat. Rev. Mol. Cell. Biol.* **2005**, *6*, 197–208.
(19) Haynes, C.; Oldfield, C. J.; Ji, F.; Klitgord, N.; Cusick, M. E.; Radivojac, P.; Uversky, V. N.; Vidal, M.; Iakoucheva, L. M. *PLoS Comput. Biol.* **2006**, *2*, e100.

Current computational design technologies, however, target structurally well defined and stable interfaces.[20,21] To address this limitation, we implemented a computational design framework that searches sequence space for binding specificity and samples both backbone and side-chain conformational space for structural optimization of the binding interface. In this study, we validated the approach on a model system by designing specific peptide inhibitors to the marginally stable coiled-coil domain of the essential yeast septin, Cdc12p. The septins comprise a family of eukaryotic proteins that perform crucial roles in cell division and cytoskeletal organization.[22] They function as heterooligomeric complexes that can form supramolecular structures (i.e., filaments). Most septins are predicted from sequence to bear a C-terminal coiled coil domain whose functions remain elusive.

Materials and Methods

Rational Design. A peptide (named anti-Cdc12pat for pattern based design) complementary to the Cdc12 wild-type, predicted coiled-coil sequence (WT Cdc12cc) was designed based on the statistical, pattern-based method used previously to create a specific probe to the coiled coil domain of the APC tumor suppressor protein.[3] This method was derived by analysis of the covariation in the core residues of the obligate, heterodimeric, cytokeratin coiled coils. Two simple patterns for heterospecificity were observed: (1) heterotypic hydrophobic contacts at positions a−a′ and d−d′; (2) complementary and repulsive charges at positions e−e′ and g−g′. To design the anti-Cdc12pat peptide, we followed these empirical rules and made 10 mutations in the last 39 residues of Cdc12 predicted by the program Multicoil to form a homodimeric coiled coil.[1] Five core-position changes—Ile3Ala, Leu14Ile, Ile17Ala, Val21Ala, Val28Ala—were chosen to alleviate core packing defects or steric clashes in the wild-type or anti-Cdc12pat homodimers. Five changes at edge e and g positions—Asn11Glu, Asp13Lys, Gln18Lys, Lys34Glu, Lys39Glu—were chosen to form favorable ion pairs upon heterodimerization with WT Cdc12cc and to destabilize anti-Cdc12pat homodimers.

Computational Design. General Scheme. To circumvent the absence of high-resolution structural information on Cdc12p WT, we implemented a computational design strategy that searches both sequence and structure space for optimized heterospecific binding interfaces (Figure 1). The method alternates between fixed-backbone sequence/side-chain-rotamer optimization and backbone/side-chain conformational optimization of the binding interface for the best designed sequences.

Structure Optimization of the Binding Interface for the WT and Designed Sequences. The structure optimization protocol samples continuously the conformational space of side-chain atoms and that of backbone atoms restricted to parametric curves defining backbone structural variation within the coiled coil fold space.[23] Initial models of the WT Cdc12cc homodimer that sample a wide range of coiled-coil superhelical parameters (i.e., radius, a-position orientation angle, frequency) were selected among the lowest energy models generated by this protocol. These models were used as initial structures for the fixed-backbone sequence design step of the first cycle. After each sequence design step, the same structure optimization protocol was applied to the designed sequences with the highest predicted stability and heterospecificity and the resulting structures were selected as initial backbone conformations for the next
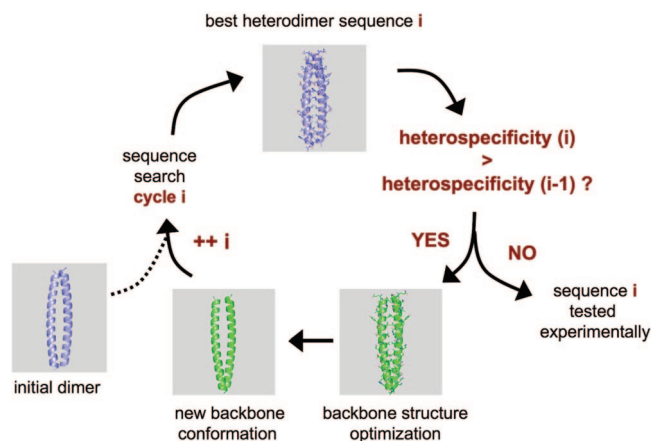
Figure 1. Schematic description of the design algorithm combining fixed-backbone sequence search for heterospecificity and backbone, side-chain conformational optimization of the best selected sequences.

sequence design cycle. This procedure was repeated until no improvement in computed heterospecificity was observed (Figure 1). Then, the sequences with the highest predicted stability and heterospecificity were subjected to the refinement protocol.

Sequence Selection for Binding Heterospecificity. Our procedure to select amino-acid sequences for binding heterospecificity is adapted from that introduced by Havranek and Harbury.[10] The method is based on a multistate design algorithm that performs both positive and negative design. In this method, we simultaneously evaluated the energies of each given sequence in the target structure and any number of competitor states using the fixed backbone repacking self-consistent mean-field (SCMF) algorithm.[24] These energies were used to define the fitness of each sequence as the transfer free energy from the target state to the ensemble of competitor states. New sequences were selected to maximize this particular fitness function using a genetic algorithm (GA). Specifically, the target state corresponded to the heterodimer containing the WT Cdc12cc and the designed anti-Cdc12, while the two competitor states corresponded to the designed homodimers and the unfolded species. Maximizing the energy differences between the target and competitor states allowed us to directly engineer binding specificity between the WT Cdc12cc and the anti-Cdc12 species. The GA generally converged in about 100 generations. We repeated this procedure many times, 100 sequences with the highest fitness were clustered into families, and the sequence with the highest fitness in each family was selected for the backbone structure optimization step.

These calculations used a physically based potential energy function similar to the function devised for the successful design of novel coiled coil heterodimers.[10] Conformational energies were evaluated using the standard united-atom OPLS-UA molecular mechanics potential[25] with an implicit solvent model (MM/IS). The total potential energy is defined as: $U^{\text{total}} = U^{\text{Geom}} + U^{\text{LJ}} + U^{\text{MTK/SA}}$. U^{Geom} and U^{LJ} are the bonded and Lennard-Jones interaction terms from OPLS-UA. $U^{\text{MTK/SA}}$ is identical to the FDPB/SA solvation energy with the electrostatic energy computed by the modified Tanford-Kirkwood algorithm (MTK).[26] The free energy of the unfolded state was evaluated in two steps: repacking the rotamers on an isolated helix followed by unfolding of the isolated helix evaluated with AGADIR.[27] We chose 13 "designable" positions of the coiled-coil interface where steric repulsion, poor

(20) Shifman, J. M.; Mayo, S. L. *Proc. Natl. Acad. Sci. U.S.A.* **2003**, *100*, 13274–13279.

(21) Kortemme, T.; Joachimiak, L. A.; Bullock, A. N.; Schuler, A. D.; Stoddard, B. L.; Baker, D. *Nat. Struct. Mol. Biol.* **2004**, *11*, 371–379.

(22) Weirich, C. S.; Erzberger, J. P.; Barral, Y. *Nat. Rev. Mol. Cell. Biol.* **2008**, *9* (6), 478–489.

(23) Harbury, P. B.; Tidor, B.; Kim, P. S. *Proc. Natl. Acad. Sci. U.S.A.* **1995**, *92*, 8408–8412.

(24) Koehl, P.; Delarue, M. *J. Mol. Biol.* **1994**, *239*, 249–275.

(25) Jorgensen, W. L.; Tiradorives, J. *J. Am. Chem. Soc.* **1988**, *110*, 1666–1671.

(26) Havranek, J. J.; Harbury, P. B. *Proc. Natl. Acad. Sci. U.S.A.* **1999**, *96*, 11145–11150.

(27) Lacroix, E.; Viguera, A. R.; Serrano, L. *J. Mol. Biol.* **1998**, *284*, 173–191.

Table 1. WT Cdc12cc, Cdc3, and Designed Anti-Cdc12 Coiled-Coil Sequences[a]

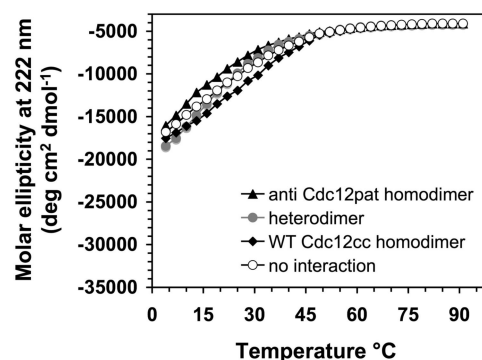| Coiled-coil sequences	
A.	1 3 7 10 14 17 21 24 28 31 35 38
B.	d a d a d a d a d a d
C.	Ac-QNIVNERIRLNYDLEEIQGKVKKLEEQVKSLQVKKSHLK-Am
D.	Ac-QNAVNERIRLEYKIEEAKGKAKKLEEQAKSLQVEKSHLE-Am
E.	Ac-QNEVNERIRLLYDLQERYGKVKKLQEQVKSLQVDISHLE-Am
F.	Ac-EKKLQKSETELFARHKEMKEKLTYQLKALEDKKKQLELSINSAS-Am

[a] The **a** and **d** positions are bold; designed positions are underlined and sequence changes are colored in red, blue and green for changes at core and edges and surface positions, respectively. **A.** Residue numbers shown for core positions **a** and **d**. **B.** Predicted assignment of the heptad repeat to the core residues by the program Multicoil. **C.** Predicted WT Cdc12cc coiled coil. **D.** Anti-Cdc12pat peptide designed using the statistical patterns discovered in the APC probe design.[3] The complementary sequence was chosen manually to alleviate core-packing defects and electrostatic repulsion in the homodimers. **E.** Anti-Cdc12comp peptide chosen by the computational algorithm combining multi-state design and backbone conformational optimization. The N- and C- terminal of each peptide were acetylated (Ac) and amidated (Am), respectively. **F.** Predicted WT Cdc3 coiled coil.

van der Waals packing and electrostatic strain were observed in the homodimeric coiled-coil models. Nineteen amino acids (excluding Pro) were allowed at these positions, and the other side chains were allowed to adopt any rotamer. We used the "penultimate", backbone-independent, rotamer library expanded by 1.23σ in χ_1 and χ_2.[28] Proton rotamers for Ser, Thr, Cys, and Tyr were added to give a total of 1058 members.

Refinement of the Selected Sequences. The fitness of each selected design sequence was cross-validated with a more accurate energy function which, in particular, computes solvation energies with the Finite Difference Poisson−Boltzmann method, FD-PB_MF.[29] Unlike the MTK potential, FDPB_MF explicitly models the effects of any changes in the molecular surface of the protein and computes accurately multibody protein−solvent electrostatic energies. A round of design calculation was performed for each selected sequence with this energy function to refine the solutions obtained with the MTK potential and to find an optimal combination of polar residues at the edge positions e and g.

Experimental Tests. Peptide Synthesis and Purification. N-terminally acetylated WT peptides (corresponding to the last 39 residues of Cdc12p and to the last 44 residues of Cdc3 predicted by the Multicoil program to exhibit strong dimeric coiled-coil propensity) and designed peptides were synthesized using solid-phase methodology with an Applied Biosystem 431A automated syntheziser. The peptides were purified using reversed phase HPLC on a semipreparative C18 column (Vydac, CA) using a linear gradient of acetonitrile in water containing 0.1% TFA. After lyophilization, the sequence and purity of the peptides were confirmed by electrospray mass spectrometry. Peptide concentrations were determined by tyrosine absorbance in 6 M guanidinum HCl.[30]

Circular Dichroism Measurements. CD studies were performed with an Aviv model 62DS spectrophotometer. Spectra were measured between 200 and 300 nm at either 1 or 20 °C with 60, 180 or 400 μM peptide in a 1 mm cuvette. Buffers used were either 20 mM potassium phosphate (pH 7) or potassium acetate (pH 5), 100 mM potassium fluoride. Thermal denaturations were measured at 222 nm from 4 to 91 °C in steps of 3 °C (2 min equilibration, 30 s data averaging). The reversibility of the thermal transitions was verified for each peptide and was found to be >90%. Due to the lack of baselines at low temperature for most species and to the lack of structural specificity of Cdc12WT, the Tm values were

(28) Lovell, S. C.; Word, J. M.; Richardson, J. S.; Richardson, D. C. *Proteins* **2000**, *40*, 389–408.
(29) Barth, P.; Alber, T.; Harbury, P. B. *Proc. Natl. Acad. Sci. U.S.A.* **2007**, *104*, 4898–4903.
(30) Edelhoch, H. *Biochemistry* **1967**, *6*, 1948–1954.

Figure 2. The predicted Cdc12 coiled coil is unstable and does not bind preferentially to the rationally designed anti-Cdc12pat peptide. Thermal melts monitored at 222 nm at pH 7.0 for 63 μM of the following species: WT Cdc12cc homodimer, anti-Cdc12pat homodimer, heterodimer (1:1 mixture of WT and anti−Cdc12pat peptide), simulated signal for the absence of heterodimerization.

not calculated by fitting the data to a particular folding model. Instead, apparent Tms were determined as the maximum of the first derivative of the CD signal at 222 nm with respect to T^{-1}.

Equilibrium Sedimentation. Equilibrium sedimentation experiments were performed using a Beckman XL-A ultracentrifuge equipped with absorbance optics and a Beckman AN-50 rotor. Samples were extensively dialyzed against 20 mM potassium phosphate buffer (pH 7), 100 mM KCl and loaded at three concentrations of peptide (50, 150, 300 μM) into a six-hole centerpiece and centrifuged at 40000 or 50000 rpm for at least 24 h at 4 and 20 °C. Five data sets averaged over 16 scans were collected at 230, 250 and 280 nm. The data sets were fitted to single molecular masses of monomer, dimer and trimer.

Results

WT Cdc12cc Coiled-Coil Stability and Modeling. The program Multicoil identified the region of *S. cerevisiae* Cdc12p between residues 369 and 407 to have a strong propensity to fold as a dimeric coiled coil[1] (Table 1). As measured by circular dichroism and equilibrium ultracentrifugation (Figure 2 and Table 2), however, the predicted Cdc12 coiled coil sequence (Cdc12cc) was only marginally helical at physiological temperature. At neutral pH and a peptide concentration of 50 μM, the WT Cdc12cc peptide showed an apparent Tm of 25 °C. This Tm, which must be taken as an upper estimate due to the absence of a lower baseline, suggests that the Cdc12cc sequence

Table 2. WT Cdc12cc/anti-Cdc12comp Complex is Helical, Thermally Stable, and Specific[a]

| peptide	apparent MW (Da)	MW/monomer mass	apparent T_m (±2 °C)	% helix at 1 °C	% helix at 37 °C
WT Cdc12cc (50 μM)	10,200	2.15	25	47	23
WT Cdc12cc (300 μM)	14,500	3.06	49	65	47
Anti-Cdc12comp (300 μM)	7,800	1.65	11	73	30
No interaction			30 (300 μM)		
WT Cdc12cc/ Anti-Cdc12comp (50 μM)	8,600	1.81	35	75	41
Cdc12 WT/Anti-Cdc12comp (300 μM)	10,300	2.17	56	85	69
Heterospecificity ΔT_m = 26 °C at 300 μM					

[a] Molecular weights were analyzed by equilibrium ultracentrifugation (see Methods). The apparent thermal melting temperature, T_m, was determined by CD at 222 nm for 50 or 300 μM total peptide concentration of WT Cdc12cc, anti-Cdc12comp or an equimolar mixture of WT Cdc12cc and anti-Cdc12comp. Helix fractions at 1 and 37 °C were calculated assuming a molar ellipticity at 222 nm of −34000 deg-cm²-dmol⁻¹ for 100% helix. Heterospecificity between the WT Cdc12cc and anti-Cdc12comp peptides was determined using the expression, $\Delta T_m = T_m^{WT/anti} - 0.5*(T_m^{WT} + T_m^{anti})$ calculated using the data obtained at 300 μM total peptide concentration.

would be natively unfolded in the absence of additional stabilizing interactions at physiological temperature.

Rational Design Strategy. Encouraged by previous successes using pattern-based design of coiled coil interfaces,[3,31] we tested the ability of covariation patterns in heterodimeric keratin coiled coils[3] to guide the design of a stable partner for Cdc12p. A 39-residue sequence called anti-Cdc12pat (Table 1) was chosen that embodies patterns found in heterodimers. Compared to the WT Cdc12cc sequence, anti-Cdc12pat contained 10 changes that were predicted to stabilize a heterodimer by alleviating unfavorable core packing and electrostatic interactions in the homodimers. The apparent melting temperature of the mixture was close to that predicted in the absence of heterotypic interactions (Figure 2), indicating that anti-Cdc12pat and WT Cdc12cc did not form a stable binding interface. The mixture also showed no excess helix formation compared to the sum of the individual peptides (Figure 2, Table 2). These results suggest that the qualitative method of sequence selection, which is effective for regular coiled coils, probably failed to account for the noncanonical context dependence of interactions at the WT Cdc12cc interface. The results highlight the need for an objective, computational, rigorous approach to the selection of molecular interactions.

Computational Design of a Cdc12p Partner. A method was developed to provide a solution to the problem of efficiently sampling flexibility at protein–protein interfaces and sequence space for binding heterospecificity in computational design calculations (Figure 1, see Methods). Briefly, the computational design method consisted of three main steps. First, an ensemble of dimeric coiled-coil structures sampling a wide range of possible coiled-coil conformations was generated for the WT Cdc12cc sequence. Second, each of these structures was selected as an initial backbone conformation of the coiled-coil interface. A first cycle of fixed-backbone/discrete side-chain rotamer selection was performed at 13 positions to select sequences optimized for binding heterospecificity. Conformations of both backbone and side-chain atoms were then optimized for the most specific predicted sequences, and the resulting structures were selected as new backbone conformations of the coiled-coil interface for another cycle of sequence selection. This sequence-

(31) Woolfson, D. N. *Adv. Protein Chem.* **2005**, *70*, 79–112.
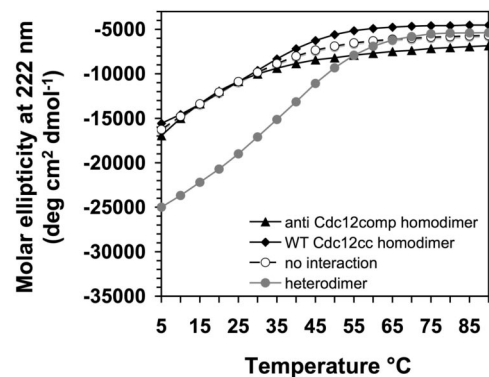
Figure 3. The computationally designed anti-Cdc12comp peptide binds specifically to the WT target. Thermal melts monitored at 222 nm at pH 7.0 for 50 μM of the following species: anti-Cdc12comp homodimer, WT Cdc12cc homodimer, heterodimer (1:1 mixture of WT and complementary peptide), simulated signal for the absence of interaction between the designed and WT species.
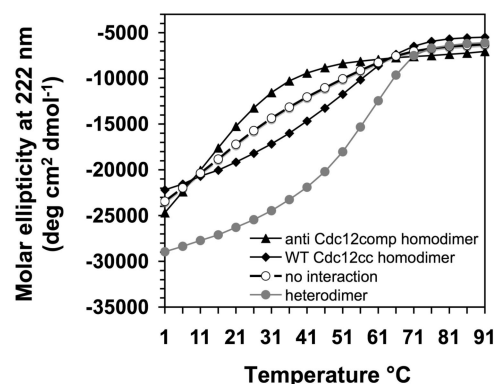
Figure 4. The computationally designed anti-Cdc12comp peptide binds specifically to the WT target. Thermal melts monitored at 222 nm at pH 7.0 for 300 μM of the following species: anti-Cdc12comp homodimer, WT Cdc12cc homodimer, heterodimer (1:1 mixture of WT and complementary peptide), simulated signal for the absence of interaction between the designed and WT species.

selection and structure optimization protocol was repeated until no improvement in computed heterospecificity was observed (Figure 1). Finally, the best sequences were refined with a more accurate energy function (see Methods). Table 1 shows the designed sequence that exhibited the highest computed heterospecificity after the structure refinement step.

The computationally designed anti-Cdc12comp sequence contained nine changes from the WT Cdc12cc. Circular dichroism and equilibrium ultracentrifugation measurements demonstrated the interaction of the target and designed peptides (Figure 3, Figure 4, Table 2). At 50 μM total peptide concentration, the equimolar mixture of the target and designed complementary peptides showed nearly 1.6-fold greater helix formation at 5 °C compared to the isolated peptides. The T_m of the mixture also showed a large increase compared to the average of the individual peptides, but the lack of lower baselines due to the unstable nature of the isolated WT Cdc12cc and anti-Cdc12comp oligomers made it difficult to quantify the heterospecificity.

To overcome this problem, the measurements were carried out at a higher total peptide concentration of 300 μM (Figure 4). At this concentration, the equimolar mixture of the anti-Cdc12comp and WT Cdc12cc sequences formed a heterodimer more stable (apparent T_m = 56 °C) and more helical (~85% at
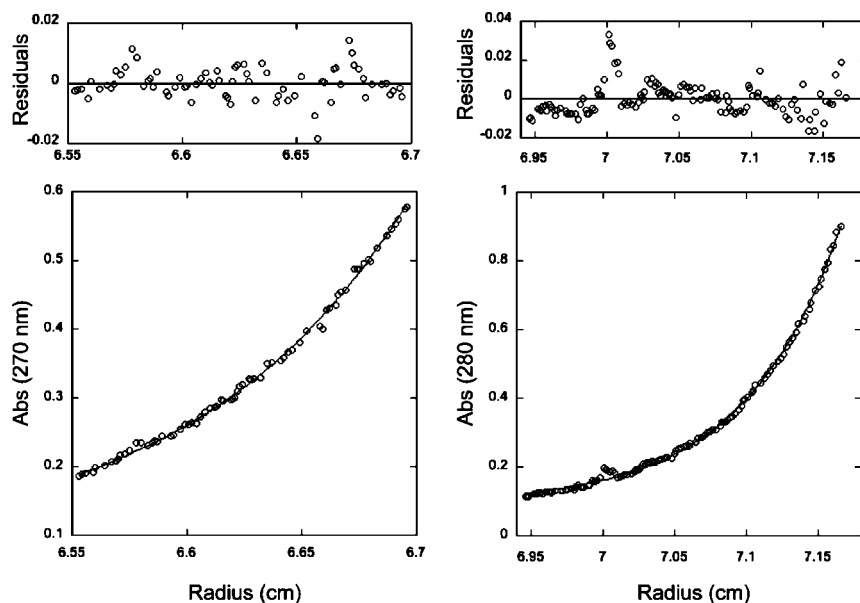
Figure 5. Representative equilibrium ultracentrifugation measurements for the designed anti-Cdc12comp alone (left panel) and for an equimolecular mixture of the anti-Cdc12comp and WT Cdc12cc peptide (right panel). The data for the designed anti-Cdc12comp are best fitted with a species of MW in between that of a monomer and that of a dimer ($1.65 \times$ monomer mass). The data for the equimolecular mixture of the anti-Cdc12comp and WT Cdc12cc peptide are best fitted with species of MW very close to that expected for a heterodimer ($2.17 \times$ monomer mass). Residuals of the corresponding fit are shown at the top of each panel.

1 °C) than either of the homodimers. Qualitatively, the peptides were more helical and denatured at higher temperatures at higher concentration, consistent with the formation of helical oligomers. While the increased peptide concentration did not resolve the folded baselines, particularly for the individual peptides, we estimated that the anti-Cdc12comp sequence bound the WT Cdc12cc target with a heterospecificity (ΔT_m) of 26 °C.

Equilibrium ultracentrifugation measurements (Figure 5, Table 2) indicated that the apparent molecular weight of the WT Cdc12cc peptide was consistent with both dimeric (50 μM) and trimeric species (300 μM). The mixture of the computationally designed and WT sequences, however, showed higher structural specificity, with an apparent molecular weight consistent with a dominant heterodimer (Figure 5, right panel). The observed increase in heterodimer stability with increasing peptide concentrations also suggests that the WT and designed sequences interact and form oligomers. These results are consistent with the intended stabilization of a specific heterodimeric helical interface. Heterospecificity was also achieved by destabilizing the designed homodimer. Both thermal melts (Figure 4, Table 2) and equilibrium ultracentrifugation measurements (Figure 5, left panel) confirm that this species is only partially folded at the measured temperatures.

To explore the molecular origins of the poor stability and low helicity of the WT Cdc12cc sequence and the potential basis for the heterospecificity of the computational design, we modeled the homo- and heterodimeric coiled coils in a family of parametrized backbone structures (see Methods). The presence of several regions with predicted steric repulsions, poor van der Waals packing and electrostatic strain is consistent with the inability of the WT Cdc12cc peptide to fold into a stable canonical coiled coil. These structural features are unusual in homodimeric coiled coils.

In contrast, our computational design method identified context-specific, sequence/structure motifs predicted to confer stability or heterospecificity. Figure 6 shows particular designed structural motifs predicted to stabilize the heterodimeric inter-
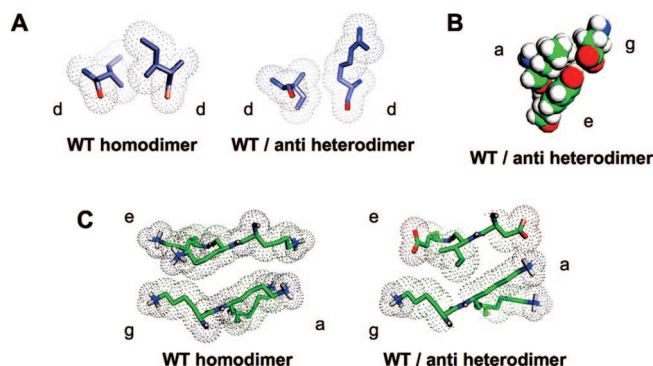
Figure 6. Designed structural motifs computationally predicted to stabilize the heterodimeric interface. (A) (Left panel) Ile17 at d is not well accommodated in the WT homodimer and induces steric repulsion. (Right panel) Ile17 was substituted for Arg in the designed anti-Cdc12comp peptide. The Arg forms good packing with the WT Ile17 in the heterodimer. The motifs are represented from the side of the coiled coil. (B) Gln18 at e was substituted by Tyr in the designed anti-Cdc12comp peptide. Tyr18 packs well with Leu14 in the predicted heterodimer, protects Leu14 from the solvent and forms an optimized hydrogen bond with Asp13 at g in the WT partner. The motifs are represented from the side of the coiled coil. (C) (Left panel) C-terminal end of the peptide is characterized by electrostatic repulsions and poor packing between Lys34, Lys35 and Lys39 in the WT homodimer. (Right panel) Lys34, Lys35 and Lys39 were substituted in the designed anti-Cdc12comp peptide by Asp, Ile and Glu, respectively. The substitutions provided better packing and electrostatic complementarity between the designed and the WT monomers. The motifs are represented from the end of the coiled coil.

face. Ile17 at d, not well accommodated in the WT Cdc12cc homodimer (Figure 6A, left panel), was substituted with Arg, which packs well with the WT Ile17 in the heterodimer (Figure 6A, right panel). Gln18 at e was substituted with Tyr, which packs well with Leu14 on the designed peptide, protects it from the solvent and forms an optimized hydrogen bond with Asp 13 at g on the WT monomer (Figure 6B). The C-terminal end of the peptide is characterized by electrostatic repulsions and poor packing of Lys 34, 35 and 39 in the WT homodimer
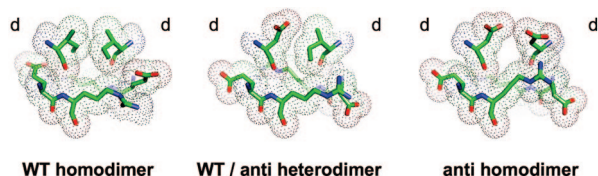
Figure 7. Computationally designed structural motifs predicted to confer heterospecificity by promoting instability of the designed homodimer (negative design). (Left panel) N-terminal Ile3 at d packs poorly in the WT homodimer. (Middle panel) Ile3 was substituted with Glu, which packs well with Ile3 and is well solvated in the heterodimer. (Right panel) Glu3 at d destabilizes the anti-Cdc12comp homodimer by poor packing and electrostatic repulsion. The motifs are represented from the side of the coiled coil.

Figure 8. The predicted Cdc3 coiled coil is unstable and does not bind strongly to the Cdc12 coiled coil. Thermal melts monitored at 222 nm at pH 7.0 for 50 μM of the following species: WT Cdc12cc homodimer, WT Cdc3cc homodimer, heterodimer (1:1 mixture of WT Cdc12cc and WT Cdc3cc peptides), simulated signal for the absence of heterodimerization.

(Figure 6C, left panel). Lys34, Lys35 and Lys39 were substituted with Asp, Ile and Glu, respectively, providing better packing and electrostatic complementarity between the designed and the WT monomers (Figure 6C, right panel). The N-terminal Ile3 at d packs poorly in the WT homodimer (Figure 7, left panel). Ile3 was substituted with Glu, which packs well and is well solvated in the heterodimer (Figure 7, middle panel). Therefore, this substitution is not expected to destabilize the heterodimer. However, as shown in the right panel, Glu3 at d destabilizes the predicted anti-Cdc12comp homodimer by promoting poor packing and electrostatic repulsion, thereby contributing to binding heterospecificity. The Ile3Glu and Ile17Arg substitutions placed charged residues at core d positions, making these design features impossible to predict using any qualitative, pattern-based criteria. Only a quantitative modeling approach that takes account of the context of each residue could have predicted these residues.

The results obtained from analytical ultracentrifugation suggest that WT Cdc12cc preferentially folds as a trimer at high peptide concentration. Ile at d is known to be better accommodated in trimers than in dimers. However, initial modeling of the trimeric state indicated that the Lysines at positions a, g and e at the C-terminus of the peptide would be less well accommodated in a trimer than in a dimer due to larger electrostatic repulsion. This predicted repulsion may explain why trimers only form at high concentrations. We focused our study on the dimeric state because it represents the easiest oligomeric state that can be targeted by the design. A similar strategy could be used to target the trimeric state and design specific heterotrimers. However, the number of interactions and alternative states to explicitly model during the design would be computationally more complex.

Comparison between the Designed (anti-Cdc12comp) and the Natural Partner (Cdc3) of Cdc12. The deletion of the C-terminal domain of Cdc12 comprising the predicted coiled coil was shown to impair the function of Cdc12 and its association with the essential Cdc3.[32] These results prompted us to analyze the strength of the interactions between the predicted coiled-coil regions of these septin isoforms. WT Cdc3 coiled coil is largely unfolded at physiological temperature (Figure 8). Association of WT Cdc3 and Cdc12 coiled-coil peptides was weak and only observable at low temperature as evidenced by a 6% increase in helicity at 4 °C of the mixture between WT Cdc12cc and WT Cdc3cc compared to that expected in absence of interaction. These results demonstrate
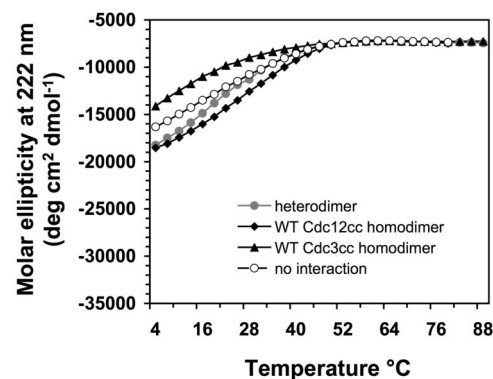
that the designed interactions between WT Cdc12cc and anti-Cdc12comp are significantly stronger than those between the predicted coiled-coil regions of Cdc12 and its natural partner Cdc3. The absence of sequence homology between WT Cdc3cc and anti-Cdc12comp (Table 2) confirms that the design method identified novel interaction motifs not selected by nature at the Cdc12/Cdc3 interface.

Discussion

Targeting and inhibiting partially disordered protein domains that lack intrinsic structural stability is an important but unsolved challenge. To address this problem, we implemented a computational design strategy that selects sequences for binding heterospecificity and searches for the optimal structures of the binding interfaces (Figure 1). This strategy was validated with the design of a specific inhibitor to the metastable coiled-coil domain of the essential yeast septin Cdc12p. Nine mutations were introduced in the WT Cdc12cc sequence to generate a designed sequence predicted to bind stably and specifically to the WT target. Specific binding of the designed sequence was demonstrated by circular dichroism and equilibrium ultracentrifugation (Figures 3–5, Table 2). As measured by the difference in estimated melting temperatures between the heterodimer and homo-oligomeric species, the designed sequence binds the Cdc12 WT target with a heterospecificity of 26 °C. This value can be considered a lower bound, owing to the uncertainty in estimating the Tm values of the metastable homodimers. Equilibrium ultracentrifugation confirmed the dimeric state of the designed binding interface. The increased helix formation and stability of the heterodimer compared to the homo-oligomers are consistent with the intended stabilization of a helical binding interface.

The coiled coil is a widespread, simple oligomerization motif and has been engineered extensively to test our understanding of the physical principles underlying molecular recognition. Most of these studies, however, focused on structurally well-defined and regular coiled-coil motifs that exhibit periodic hydrophobic/polar sequence patterns for which core packing complementarity and optimized electrostatic interactions at the edges are expected to promote stability and specificity.[3,31,33] While rational and sequence-based design strategies were

(32) Versele, M.; Gullbrand, B.; Shulewitz, M. J.; Cid, V. J.; Bahmanyar, S.; Chen, R. E.; Barth, P.; Alber, T.; Thorner, J. *Mol. Biol. Cell* **2004**, *15*, 4568–4583.

(33) Mason, J. M.; Schmitz, M. A.; Muller, K. M.; Arndt, K. M. *Proc. Natl. Acad. Sci. U.S.A.* **2006**, *103*, 8989–8994.

successful for these systems, a similar approach applied to the Cdc12 coiled coil failed to predict sequences that bind to the target (Figure 2). This result suggests that, when the sequence of the coiled-coil target starts to deviate significantly from canonical sequence pattern, more objective design strategies are needed to account for specific sequence context effects. By modeling limited backbone and complete side-chain flexibility, our computational approach identified combinations of nonpolar and polar interactions that stabilize the noncanonical coiled-coil motifs of the Cdc12 WT sequence into a heterodimeric helical interface. Several structural motifs were selected in our designs that are not found in regular coiled coils. These features include, for example, Ile3Glu, Ile17Arg and Gln18Tyr. The first two of these replacements at core d positions are predicted to accommodate the disfavored Ile in the WT partner sequence and optimize the solvation and the structural specificity of the heterodimers (Figures 6 and 7). Tyr18 at position e is predicted by the structural model to protect a core residue from the solvent and optimizes a salt bridge across the interface (Figure 6B). The heterospecificity of 26 °C of the computationally designed, anti-Cdc12 sequence for its target compares well with that obtained with rational design and evolution approaches on regular coiled coils.[3] We also observed a 20% increase in helix formation and stability ($\Delta T_m = 7$ °C) of the heterodimer compared to WT Cdc12cc. However, these values are relatively modest compared to the increase in stability obtained recently by *in vivo* evolution on the Fos/Jun system.[33,34] We limited the modeling of backbone flexibility to that compatible with the coiled-coil fold as parametrized by Crick and successfully applied by Harbury[23] and later by Keating.[9] This simplified parametrization of the backbone conformational degrees of freedom does not capture local structural distortions and deviations from ideality that may be induced by the WT Cdc12cc sequence. A more general approach to sampling of local sequence/structure motifs[35,36] may be needed to achieve greater stability and heterospecificity.

Several studies identified Cdc3 as an essential physiological partner of Cdc12p in budding yeast.[37] Deletions of a larger fragment containing the predicted coiled coil in both Cdc12 and Cdc3 were shown to impair septin associations and function.[32] However, our analysis of the isolated coiled coils indicates that these isolated domains do not significantly associate under physiological temperature (Figure 8). Sequence comparison between Cdc3 and the designed anti-Cdc12comp did not show any significant similarity (Table 1). Altogether, these results suggest that our computational strategy identified interaction motifs that are stronger than the natural Cdc12/Cdc3 coiled-coil interface. Further studies will be needed to identify the role of the region upstream to the predicted coiled coil in promoting the stability and heterospecificity of septin assemblies.

Our results set the stage for functional analysis of the role of coiled-coil domain in the function of Cdc12p *in vivo*. The recent structure of the human septin complex suggests that the coiled-coil region alone is dispensable for human septin heteroassociation and available for interactions with other partners.[38] The coiled coil domains of Cdc12p and Cdc3p have been proposed to mediate septin filament pairing coupled to elongation.[37] The ability to express the designed peptide alone or together with a fluorescent reporter in synchronized budding yeasts at specific time of the cell cycle may provide a new means to study the septin coiled-coil function in a space- and time-resolved manner. Coiled-coil domains are recurrent motifs at the C-terminus of many mammalian septins. Generalizing our engineering strategy to target the family of related septin coiled-coil domains may help to better identify the septin interactome and its specificities across species.

(34) Mason, J. M.; Muller, K. M.; Arndt, K. M. *Biochemistry* **2007**, *46*, 4804–4814.
(35) Schueler-Furman, O.; Wang, C.; Bradley, P.; Misura, K.; Baker, D. *Science* **2005**, *310*, 638–642.
(36) Kuhlman, B.; Dantas, G.; Ireton, G. C.; Varani, G.; Stoddard, B. L.; Baker, D. *Science* **2003**, *302*, 1364–1368.
(37) Bertin, A.; McMurray, M. A.; Grob, P.; Park, S.-S.; Garcia, G.; Patanwala, I.; Ng, H.-L.; Alber, T.; Thorner, J.; Nogales, E. *Proc. Natl. Acad. Sci. U.S.A.* **2008**, *105*, 8274–8279.
(38) Sirajuddin, M.; Farkasovsky, M.; Hauer, F.; Kuhlmann, D.; Macara, I. G.; Weyand, M.; Stark, H.; Wittinghofer, A. *Nature* **2007**, *449*, 311–315.